

**Table IV.** Ionization Energies of Triphenyl Derivatives of N, P, As, Sb, and Bi

compound	$I_D$ , eV <sup>a</sup>		$I_P$ , eV		
	$\lambda_1$	$\lambda_2$	$b_1$	$a_2$	$n$
Ph <sub>3</sub> N <sup>b</sup>	9.04	7.11	6.99	8.80	10.27
Ph <sub>3</sub> P <sup>b</sup>			10.90	9.25	7.88
Ph <sub>3</sub> As <sup>b</sup>	9.09	8.14	10.40	8.90	7.95
Ph <sub>3</sub> Sb <sup>b</sup>	9.00	8.09	10.09	9.14	8.18
Ph <sub>3</sub> Bi	8.91	7.99			

<sup>a</sup>  $I_D$  calculated with eq 5, ref 31. <sup>b</sup>  $I_P$  from ref 28.

amine-TCNE's are greater than unity (1.02-1.40) while  $A_2/A_1$  values for Ph<sub>3</sub>M-TCNE's are less than unity (0.34-0.60). These comparisons indicate that there is a fundamental difference in the mode of interaction of TCNE with the HOMO's of the phenylamines and those of Ph<sub>3</sub>As, Ph<sub>3</sub>Sb, and Ph<sub>3</sub>Bi.

On the basis of PES data and CNDO/2 calculations, Debies and Rabalais<sup>28</sup> concluded that the energies of the highest occupied orbitals in phenylamines decreased in the order  $b_1 > a_2 > n$ , whereas the energies of the highest occupied orbitals in Ph<sub>3</sub>M compounds decreased in the order  $n > a_2 > b_1$ . They attributed this reversal of  $n$  and  $b_1$  orbital energies primarily to shifts of electron density to the central atom by  $p\pi \rightarrow d\pi$  interactions in the Ph<sub>3</sub>M compounds, which result in an increase of the electron density on the central atoms in the order  $N < Sb < As < P$ .

The correlation of  $I_P$  values of Ph<sub>3</sub>N, Ph<sub>3</sub>As, and Ph<sub>3</sub>Sb with  $I_D$  values of the corresponding TCNE complexes (Table IV) suggests that  $\lambda_1$  bands in Ph<sub>3</sub>N-TCNE and Ph<sub>3</sub>M-TCNE complexes arise from an  $a_2$  transition, whereas the  $\lambda_2$  bands arise from delocalized  $b_1$  orbitals in phenylamine-TCNE's and from localized  $n$  orbitals in Ph<sub>3</sub>M-TCNE's. This difference in the nature of the HOMO of the phenylamines ( $b_1$ ) and Ph<sub>3</sub>M compounds ( $n$ ) apparently gives rise to the differences in the  $\lambda_2$  bands for the TCNE complexes of these two classes of compounds. The observed trends in electron density on the central atoms of these compounds are consistent with the reactivity of TCNE with Ph<sub>3</sub>P and the triarylphosphines relative to triaryl derivatives of N, As, Sb, and Bi if it is assumed that the reaction depends upon the interaction

of the highly electrophilic TCNE with a negatively charged central atom.

The structure of Ms<sub>3</sub>P and its behavior toward TCNE are of interest in this connection. A structural study<sup>38</sup> of Ms<sub>3</sub>P indicates a mean bond angle  $\angle CPC$  of 109.7° compared to 103° for Ph<sub>3</sub>P. The extraordinary flattening of Ms<sub>3</sub>P is attributed to strong steric repulsions between *o*-methyl groups on adjacent rings which incidentally almost completely shield the phosphorus atom. The very low rate of reaction of Ms<sub>3</sub>P and TCNE is probably due to the inability of TCNE to interact effectively with the  $n$  electrons of the hindered phosphorus atom. Consequently, the formation of Ms<sub>3</sub>P-TCNE must involve a charge-transfer interaction between TCNE and either or both of the  $a_2$  and  $b_1$  orbitals of the mesityl groups. The spectrum of Ms<sub>3</sub>P-TCNE consists of a single band with  $\lambda_{max}$  416 nm. The related complexes MsH-TCNE<sup>9</sup> and Ms<sub>3</sub>B-TCNE also have single bands with  $\lambda_{max}$  461 and 475 nm, respectively. The lower  $\lambda_{max}$  value of Ms<sub>3</sub>P-TCNE is expected because of electron withdrawal from the rings through  $p\pi \rightarrow d\pi$  interactions.

In summary, the chemical behavior of TCNE with aryl derivatives of group 15 elements and the characteristics of their complexes indicate that (1) the lowest energy CT transitions between TCNE and arylamines involve the  $b_1$  and  $a_2$  orbitals on the aromatic ring which are energized by  $n \rightarrow \pi$  conjugation, (2) the lowest energy CT transitions between TCNE and aryl derivatives of P, As, Sb, and Bi generally involve the  $n$  electrons on the central atom which are energized by  $p\pi \rightarrow d\pi$  conjugation, and (3) the rate of irreversible reactions of TCNE with group 15 aryls is influenced by the magnitude of the negative charge on the central atom and its steric accessibility.

**Acknowledgment.** We are grateful for financial support from the Peter White Fund and the Ellen K. Russell Trust Fund of Northern Michigan University. We are indebted to Dr. Gerald D. Jacobs, Dr. David Kingston, Dr. Jerome A. Roth, and Dr. Philip I. Pavlik for valuable discussions, to Dr. R. I. Walter for the gift of a compound, and to Susan R. Lang for technical assistance.

## Chemical Reactions on Clusters. 4. Gas-Phase Unimolecular Decomposition of the Acetone and Acetone-*d*<sub>6</sub> Ions in Association with Argon and Carbon Dioxide Clusters

A. J. Stace

Contribution from the School of Molecular Sciences, University of Sussex, Falmer, Brighton, Sussex, U.K. BN1 9QJ. Received July 3, 1984

**Abstract:** Ion clusters of the type Ar<sub>*n*</sub>·(CD<sub>3</sub>)<sub>2</sub>CO<sup>+</sup>, Ar<sub>*n*</sub>·(CH<sub>3</sub>)<sub>2</sub>CO<sup>+</sup>, and (CO<sub>2</sub>)<sub>*n*</sub>·(CH<sub>3</sub>)<sub>2</sub>CO<sup>+</sup> for  $n$  up to 35 have been formed by electron impact following the adiabatic expansion of an inert gas/acetone mixture. In each case the acetone ion is observed to undergo unimolecular decomposition to give either X<sub>*n*</sub>·CD<sub>3</sub>CO<sup>+</sup> or X<sub>*n*</sub>·CH<sub>3</sub>CO<sup>+</sup>. Other product ions, such as CD<sub>3</sub><sup>+</sup> and CH<sub>3</sub><sup>+</sup>, which are present in the mass spectrum of the isolated ion, do not appear when acetone is clustered with either argon or carbon dioxide. Overall the product ion intensity on argon clusters is higher than that on carbon dioxide clusters. To account for these observations, a simple model is proposed in which it is assumed that unimolecular decomposition of the molecular ion and vibrational predissociation of the inert gas are in competition. Calculated results from the model suggest that the time scale for vibrational predissociation lies in the range 10<sup>-12</sup>-10<sup>-10</sup> s. Reaction products from unimolecular processes which proceed faster than 10<sup>-12</sup> s are observed, whereas products from those reactions which are calculated to take place on a time scale >10<sup>-10</sup> s are not. The experimental results indicate that the ions Ar<sub>11</sub>·CD<sub>3</sub>CO<sup>+</sup> and Ar<sub>11</sub>·CH<sub>3</sub>CO<sup>+</sup> are particularly stable, and it is suggested that this stability is due to the formation of a "magic" number atom configuration.

A number of recent experiments have exploited the fragile nature of van der Waals (vdW) molecules in order to gain some understanding of the interactions responsible for their formation and stability.<sup>1</sup> Thus, the energy of a single infrared photon is

often sufficient to bring about the "unimolecular decomposition" of a wide range of vdW molecules.<sup>2-7</sup> The mechanism for this

(1) Levy, D. H. *Adv. Chem. Phys.* 1983, 47, 323.

(2) Hoffbauer, M. A.; Gentry, W. R.; Giese, C. F. In "Laser-Induced Processes in Molecules"; Kompa, K. L., Smith, S. D., Eds.; Springer: Berlin, 1978.

decomposition is vibrational predissociation, and at low photon energies, it is probably the only deexcitation channel open to the molecule. If the energy of the photon is increased to a point where electronic excitation of a vdW molecule can occur, new deexcitation channels become accessible,<sup>1,8-10</sup> the most obvious is fluorescence. However, there is also a possibility that covalent bond fission will take place.<sup>8</sup> Although there are exceptions,<sup>8</sup> it would appear that for most of the vdW molecules studied so far, the vibrational predissociation times are considerably shorter than the time scales of any of the alternative deexcitation routes.<sup>1</sup>

If an excited vdW molecule consists of a diatom complexed with an inert gas atom, then the vibrational predissociation time will depend primarily on the magnitudes of the transition matrix elements which couple the initial and final states of the species.<sup>11-13</sup> However, in the case of a polyatomic molecule with a low density of vibrational states at the excitation energy, intramolecular vibrational relaxation (IVR) may influence events by introducing a time lag between excitation and vibrational predissociation. Vibrational energy present in the excited mode may not flow directly to that mode which is most strongly coupled to the vdW bond.<sup>1</sup> This could have the effect of reducing the vibrational predissociation time to a value where it would be comparable with other slower processes, such as fluorescence and true unimolecular decay (as typified by an RRKM molecule). Under such circumstance, two or more of the deexcitation channels could operate in competition.<sup>1</sup> Alternatively, if the internal excitation of the polyatomic molecule was sufficiently high, the relative time scale for vibrational predissociation could actually be longer than that for covalent bond fission.

In a recent series of experiments, we have begun to study the unimolecular decomposition of molecular ions in association with inert gas clusters.<sup>14-16</sup> It is anticipated that these experiments could offer an alternative means of studying vibrational predissociation because we believe the decomposition process to be in competition with the loss of inert gas atoms or molecules from the ion cluster. From our analysis of the results, it will be seen that the internal energy available to the molecular ions is of the order of 5–6 eV. Although this energy may be large compared to that necessary for the removal of a single inert gas atom, the energy loss resulting from the evaporation of many such atoms could be sufficient to suppress unimolecular decomposition. From a knowledge of the lifetime of the molecular ion with respect to each of the energetically allowed reaction channels, it should be possible to place a limit on the time scale of the vibrational predissociation process. The purpose of this paper is to present new experimental results and to use them to develop a quantitative understanding of the mechanism behind our observations.

From previous results<sup>14-16</sup> we have drawn a number of conclusions regarding the position and behavior of the reactant ion with respect to the main body of the cluster. Briefly, these conclusions are as follows: (1) in large clusters excitation of the molecular ion appears to proceed via a charge-transfer mechanism, with the internal energy of the ion being equal to the difference  $IP(\text{inert gas}) - IP(\text{molecule})$ ; (2) the molecular ion decomposes

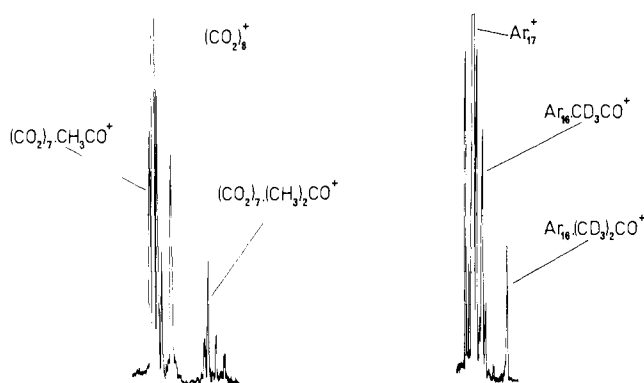


Figure 1. Typical examples of the recorded mass spectra. Also present are isotope and metastable peaks.

because of the relatively slow rate of intermolecular energy transfer between it and the inert gas component of the cluster; (3) the structural and chemical information contained within the results suggests that the product ions, and possibly the parent ions, "sit on" rather than "within" the cluster; and (4) individual clusters appear to exhibit behavior which could be associated with the inert gas component undergoing a phase transition. We believe the results presented in this paper will help to substantiate and further develop these conclusions.

### Experimental Section

Neutral clusters were generated by the adiabatic expansion of a gas mixture through a pulsed nozzle operating at approximately 20 Hz. Following collimation through a 0.5 mm diameter skimmer positioned 2 cm from the nozzle, the modulated cluster beam was ionized by electron impact and mass analyzed on a modified A.E.I. MS 12 mass spectrometer. As with previous experiments,<sup>14-16</sup> it was found necessary to maintain the acetone concentration below 100 ppm; any higher than that and the mass spectrum became dominated by acetone ion clusters. Figure 1 shows two examples of recorded mass spectra. As can be seen, the intensities of the ion peaks of interest are comparatively low. For this reason the mass spectrometer was operated with the source and collector slits set to their maximum values, which resulted in some loss of resolution.

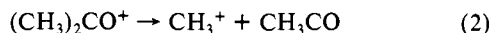
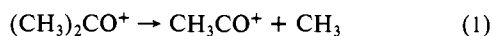
As we have tried to emphasize previously,<sup>16</sup> the low intensities of the reactant and product ions together with coincidences in the nominal mass for a number of ion clusters places limitations on the range of molecular decompositions which can be studied in detail. For this reason we have combined the results for both acetone and acetone-*d*<sub>6</sub> in order to provide a complete picture of events taking place on the clusters. Particular difficulties were encountered because of the presence of water vapor in the nozzle. Despite baking the nozzle for long periods, it was found almost impossible to reduce the water content to a level where  $Ar_n \cdot H_2O$  cluster ions no longer appeared in the mass spectra. This together with the fact that it was not possible to dry the acetone completely meant that we could not normalize the data obtained for the reactions of  $Ar_n \cdot (CH_3)_2CO^+$  clusters, the reason being that  $Ar_n \cdot (CH_3)_2CO^+$  and  $Ar_{n+1} \cdot H_2O$  have the same nominal mass. For a similar reason, it was not possible to establish the presence of  $Ar_n \cdot CD_3^+$ . In the case of carbon dioxide, we could not follow the reactions of acetone-*d*<sub>6</sub> because of a mass coincidence between  $(^{13}CO_2)_2 \cdot (CO_2)_n^+$  and  $(CO_2)_{n+1} \cdot CD_3CO^+$ , and for  $(CO_2)_n \cdot (CH_3)_2CO^+$  clusters, the reduced resolution prevented us from going beyond  $n = 19$ . Also shown in Figure 1 are metastable peaks arising from the reactions  $Ar_n^+ \rightarrow Ar_{n-1}^+ + Ar$  and  $(CO_2)_n^+ \rightarrow (CO_2)_{n-1}^+ + CO_2$ . There was considerable interference between these peaks and the product ions  $Ar_n \cdot CH_3CO^+$  below  $n = 11$ , and for the same reason it was not possible to obtain a result for  $Ar_5 \cdot CD_3CO^+$ . It should again be stressed that the ions we are attempting to study do have very low intensities, which means that peaks in the mass spectra arising from parent or product ions can quite easily be lost beneath argon or carbon dioxide isotope peaks or beneath peaks resulting from the presence of an impurity. To this extent we have found the use of isotopes as a means of cross-checking the results invaluable. All the results presented were obtained using an electron impact energy of 70 eV.

During the course of an experiment, the pressure in the expansion chamber was approximately  $1 \times 10^{-4}$  torr, in the collimation chamber it was  $1 \times 10^{-6}$  torr, and in the ion source of the mass spectrometer the pressure remained below  $1 \times 10^{-6}$  torr. The latter low value allows us to disregard the possibility that ion-molecule reactions are responsible for the effects we observe.

- (3) Gough, T. E.; Miller, R. E.; Scoles, G. *J. Phys. Chem.* **1981**, *85*, 4041.
- (4) Casassa, M. P.; Western, C. M.; Celli, F. G.; Brinza, D. E.; Janda, K. *J. Chem. Phys.* **1983**, *79*, 3227.
- (5) Geraedts, J.; Setiadi, S.; Stolte, S.; Reuss, J. *Chem. Phys. Lett.* **1981**, *78*, 277.
- (6) Miller, R. E.; Watts, R. O.; Ding, A. *Chem. Phys.* **1984**, *83*, 155.
- (7) Hoffbauer, M. A.; Giese, C. F.; Gentry, W. R. *J. Phys. Chem.* **1984**, *88*, 181.
- (8) Brumbaugh, D. V.; Kenny, J. E.; Levy, D. H. *J. Chem. Phys.* **1983**, *78*, 3415.
- (9) Halberstat, N. *Faraday Discuss. Chem. Soc.* **1982**, *73*, 400.
- (10) Halberstat, N.; Soep, B. *J. Chem. Phys.* **1984**, *80*, 2340.
- (11) Ewing, G. E. In "Intramolecular Dynamics"; Jortner, J., Pullman, B., Eds.; Reidel: London, 1982.
- (12) Ewing, G. E. *Faraday Discuss. Chem. Soc.* **1982**, *73*, 325.
- (13) Beswick, J. A.; Jortner, J. *Adv. Chem. Phys.* **1983**, *47*, 363.
- (14) Stace, A. J. *J. Phys. Chem.* **1983**, *87*, 2286.
- (15) Stace, A. J. *Chem. Phys. Lett.* **1983**, *99*, 470.
- (16) Stace, A. J. *J. Am. Chem. Soc.* **1984**, *106*, 4380.

## Results and Discussion.

In the normal mass spectrum of acetone the following ions are the most intense:  $(\text{CH}_3)_2\text{CO}^+$  ( $58^+$ ),  $\text{CH}_3\text{CO}^+$  ( $43^+$ ), and  $\text{CH}_3^+$  ( $15^+$ ). Their formation can be accounted for with the mechanism



The thermodynamics and kinetics of these two processes have been studied in some detail,<sup>17-19</sup> and a similar fragmentation pattern has been observed for acetone ion clusters.<sup>20,21</sup> When acetone was clustered with argon, the following ions were observed:  $\text{Ar}_n(\text{CH}_3)_2\text{CO}^+$  and  $\text{Ar}_n\text{CH}_3\text{CO}^+$  for  $n$  in the range 1-22. The analogous ions were also found for acetone- $d_6$ ; however, because of the increased mass separation between  $\text{Ar}_n\text{CD}_3\text{CO}^+$  and the metastable peaks resulting from the decomposition of pure argon ion clusters, it was possible to extend the observation range for acetone- $d_6$  as far as  $n = 35$ . When clustered with carbon dioxide, acetone gave the following ions:  $(\text{CO}_2)_n(\text{CH}_3)_2\text{CO}^+$  and  $(\text{CO}_2)_n\text{CH}_3\text{CO}^+$  for  $n$  in the range 1-19. Neither the argon nor the carbon dioxide systems showed any evidence of ions resulting from a reaction analogous to (2). The reaction step leading to the formation of  $\text{Ar}_n\text{CH}_3^+$  was also absent from the fragmentation pattern for  $\text{Ar}_n(\text{CH}_3)_2\text{O}^+$ .<sup>16</sup> Any consideration of the relative magnitudes of the critical energies necessary to remove either a methyl group or an argon atom from the ion clusters would suggest that the observation of the above fragment ions is quite unexpected.

Figure 2 shows the relative intensities of the reaction products from a number of different sized clusters plotted as a function of nozzle stagnation pressure. The marked pressure dependence has been noted previously,<sup>15,16</sup> and although this is again an unexpected result, it is one which has appeared consistently in all the  $\text{Ar}_n\text{X}^+$  systems studied so far.<sup>15,16,22</sup> It has been suggested that this behavior is due to a phase transition taking place in the argon component as the nozzle pressure is increased.<sup>15</sup> The fact that at sufficiently low nozzle pressures it is possible to form parent cluster ions in the absence of any reaction products is, we believe, particularly significant to the interpretation of these results. In contrast to the observed behavior for argon, the relative intensities of the reaction products on carbon dioxide clusters display almost no pressure dependence. Attempts to modify the  $\text{CO}_2$  cluster behavior through the use of mixtures with helium have so far failed.<sup>22</sup>

Figures 3-5 show the relative intensities of the product ions plotted as a function of cluster size. Each point is the average of approximately six separate measurements made at that nozzle pressure which gave the highest product ion intensity. In all three figures the results for  $n < 22$  were obtained using an ion source potential of 8 kV. In Figure 3 a potential of 5 kV was used to record the results for  $n$  in the range 22-35. The signal-noise ratios for the latter were quite low, and because of this, we do not consider the results to have any quantitative significance. However, even beyond  $n = 35$ , there was evidence of fragmentation.<sup>22</sup> It is evident from Figures 3 and 4 that the role of the argon atoms is by no means passive, with the relative intensities showing several pronounced fluctuations. It is also interesting to note that despite the experimental difficulties discussed earlier, a number of the fluctuations are common to both  $(\text{CH}_3)_2\text{CO}^+$  and  $(\text{CD}_3)_2\text{CO}^+$ . Of particular interest in this respect is the large difference in product ion intensity between  $\text{Ar}_{11}$  and  $\text{Ar}_{12}$ . In contrast to the above results, the product ion intensities on the  $\text{CO}_2$  clusters show no large fluctuations, and their relative values are lower than those observed for argon. It has been suggested<sup>16</sup> that the high product

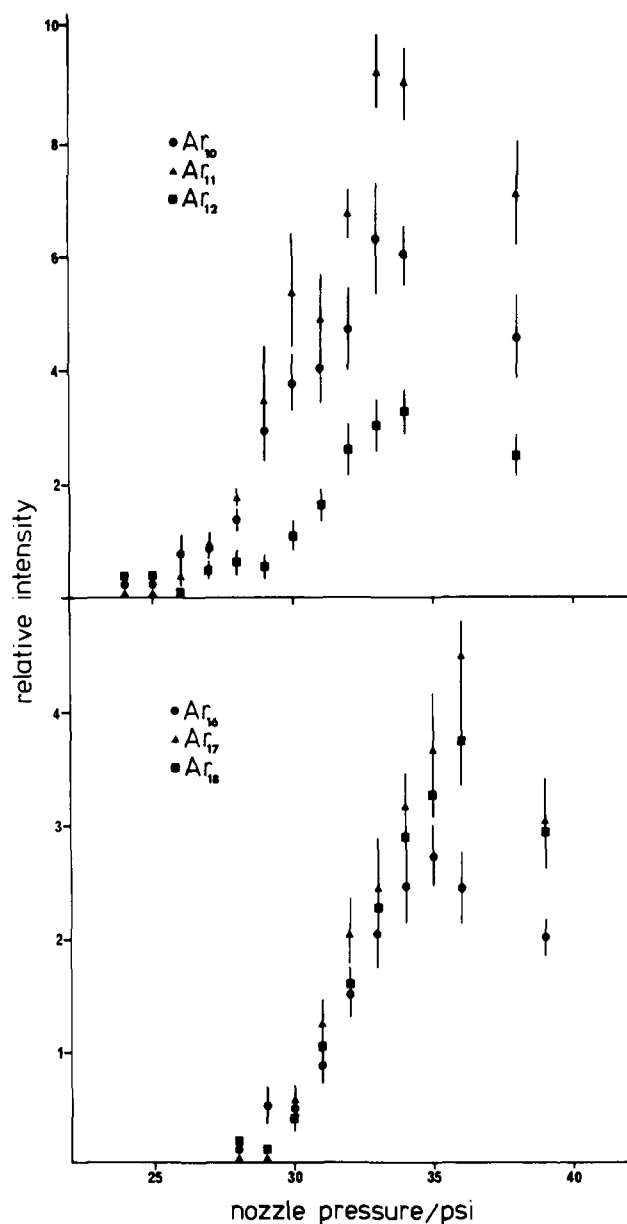


Figure 2. Relative product ion intensities as a function of nozzle stagnation pressure. For each example the intensity of the  $\text{Ar}_n\text{CD}_3\text{CO}^+$  peak has been divided by the intensity of the  $\text{Ar}_n(\text{CD}_3)_2\text{CO}^+$  peak. The error bars represent  $\pm 1$  standard deviation. Note that there is a difference in scale between the upper and lower figure.

ion intensities at small  $n$  are due to inert gas atom loss from the larger ion clusters and that below  $n = 9-10$  the intensities are unlikely to reflect the properties of individual ion clusters.

In the analysis of these and other results,<sup>14-16,22</sup> we have attempted to address three questions, they are as follows: (1) how does the molecular ion acquire sufficient energy to decompose, (2) if there is approximately 5 eV of potential energy within an ion cluster, why do the inert gas atoms remain bound to the ion (on the time scale of the experiment ( $\approx 10^{-6}$  s), extensive evaporation might have been expected), and (3) can the modified set of unimolecular reactions displayed by the molecular ion provide any information on the ion's position with respect to the inert gas component. We believe that satisfactory answers to these questions will lead to a fundamental understanding of the physics and chemistry of these systems.

From our analysis of the argon-dimethyl ether data,<sup>16</sup> it was concluded that in large ion clusters, i.e.,  $n > 9-10$ , the molecular ion was excited by a charge-transfer mechanism, through which the ion received the energy difference  $\text{IP}(\text{argon}) - \text{IP}(\text{molecule})$ . Two pieces of evidence were presented to support this conclusion; firstly, the relative intensities of product ions from large clusters

(17) Murad, E.; Inghram, M. G. *J. Chem. Phys.* **1964**, *40*, 3263.

(18) Cant, C. S. T.; Danby, C. J.; Eland, J. H. D. *J. Chem. Soc., Faraday Trans. 2* **1975**, *71*, 1015.

(19) Lifshitz, C. *J. Phys. Chem.* **1983**, *87*, 2304.

(20) Stace, A. J.; Shukla, A. K. *J. Phys. Chem.* **1982**, *86*, 865.

(21) Trott, W. M.; Blais, N. C.; Walter, E. W. *J. Chem. Phys.* **1978**, *69*, 3150.

(22) Stace, A. J., unpublished results.

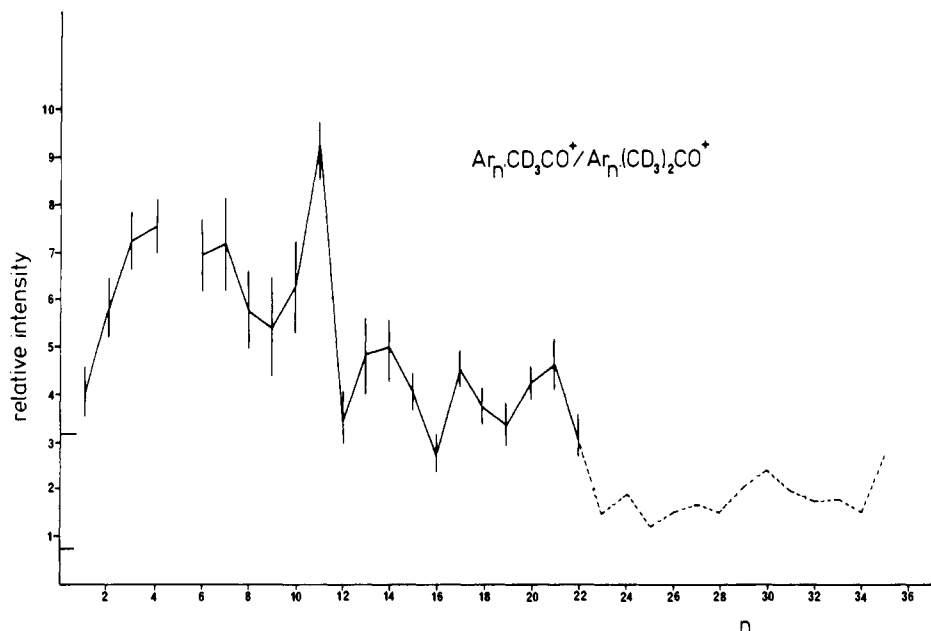


**Figure 3.** Relative product ion intensity as a function of argon cluster size for the decomposition of  $\text{Ar}_n(\text{CD}_3)_2\text{CO}^+$ . The results for  $n < 22$  were recorded with an ion source potential of 8 kV; for  $n > 22$  the source potential was reduced to 5 kV. The error bars represent  $\pm 1$  standard deviation.

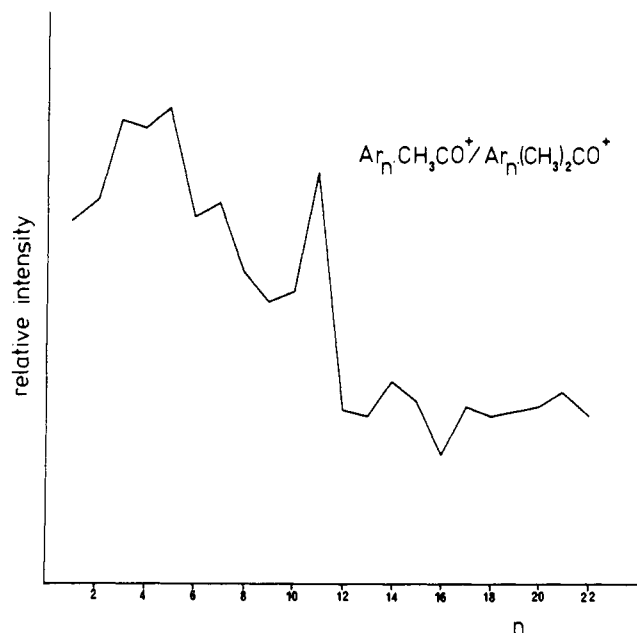


**Figure 4.** Relative product ion intensity as a function of argon cluster size for the decomposition of  $\text{Ar}_n(\text{CH}_3)_2\text{CO}^+$ . See Experimental Section for details of the difficulties associated with these particular measurements.

were almost independent of electron impact energy and, secondly, no reactions were observed for which the following relationship held:  $\text{IP}(\text{argon}) - \text{IP}(\text{molecule}) - \epsilon_0 < 0$ , where  $\epsilon_0$  is the critical energy of reaction. In the light of more recent experiments we would like to reappraise some of the results presented previously.<sup>16</sup> In particular, it has now become evident that our apparatus will not provide accurate electron impact-dependent data below 30 eV. In order to allow the cluster beam collision-free access to the ion source, it was necessary to modify the mechanism which regulates the filament. The result is that the ion source no longer has an internal reference which can operate accurately at low electron impact energies. An ion source detuning effect<sup>23</sup> which arises from the relatively high kinetic energy of the larger clusters prevents us from using inert gases to calibrate the source under

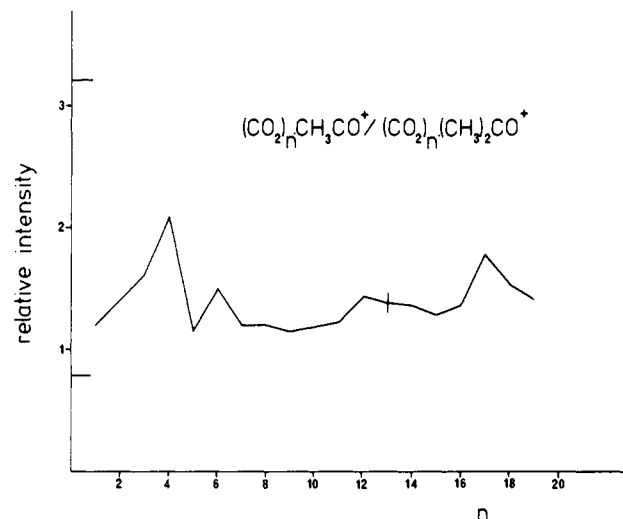


**Figure 5.** Relative product ion intensity as a function of carbon dioxide cluster size for the decomposition of  $(\text{CO}_2)_n(\text{CH}_3)_2\text{CO}^+$ . In general the errors associated with these measurements were much lower than those for the corresponding argon clusters. A typical error bar for  $\pm 1$  standard deviation is shown.

those conditions that are optimum for the observation of ion clusters. Hence, we are no longer confident that electron impact energy-dependent data from our apparatus can be used to substantiate the charge-transfer mechanism. However, the relationship given above does still hold, and we shall show later in this section that we can in fact be quite specific about the energy requirements necessary for reactivity. In considering the energetic of these systems, there is an additional factor which we have not previously taken into account, and that is that an argon cluster has a lower ionization potential than an argon atom,<sup>24</sup> the main contribution to this decrease coming from the stability of the argon dimer ion,  $\text{Ar}_2^+$ .<sup>24</sup> A small reduction in IP has also been observed for carbon dioxide clusters.<sup>25,26</sup> Thus, if the positions of the molecules vary with respect to the inert gas components, the molecular ions could be formed with a distribution of internal energies.

(23) Stace, A. J.; Shukla, A. K. *Int. J. Mass Spectrom. Ion Phys.* **1980**, *36*, 119.

(24) Dehmer, P. M.; Pratt, S. T. *J. Chem. Phys.* **1982**, *76*, 843.

(25) Jones, G. G.; Taylor, J. W. *J. Chem. Phys.* **1978**, *68*, 1768.

(26) Linn, S. H.; Ng, C. Y. *J. Chem. Phys.* **1981**, *75*, 4921.

Table I. Energetics and Unimolecular Rate Constants for Acetone Ions Excited by Charge Transfer

reaction	$\epsilon_0^a$	$E^a$		$E - \epsilon_0$		$k(E)^b$		$\approx \tau_k, s$
		Ar <sup>+</sup> c	Ar <sub>6</sub> <sup>+</sup> c	Ar <sup>+</sup>	Ar <sub>6</sub> <sup>+</sup>	Ar <sup>+</sup>	Ar <sub>6</sub> <sup>+</sup>	
(CD <sub>3</sub> ) <sub>2</sub> CO <sup>+</sup> → CD <sub>3</sub> CO <sup>+</sup> + CD <sub>3</sub>	0.61	6.06	4.56	5.45	3.95	4.6 × 10 <sup>13</sup>	3.2 × 10 <sup>13</sup>	<10 <sup>-12</sup>
(CD <sub>3</sub> ) <sub>2</sub> CO <sup>+</sup> → CD <sub>3</sub> <sup>+</sup> + CD <sub>3</sub> CO	3.31	6.06	4.56	2.75	1.25	1.6 × 10 <sup>9</sup>	1.4 × 10 <sup>7</sup>	>10 <sup>-10</sup>
(CH <sub>3</sub> ) <sub>2</sub> CO <sup>+</sup> → CH <sub>3</sub> CO <sup>+</sup> + CH <sub>3</sub>	0.61	6.06	4.56	5.45	3.95	5.2 × 10 <sup>13</sup>	3.1 × 10 <sup>13</sup>	<10 <sup>-12</sup>
(CH <sub>3</sub> ) <sub>2</sub> CO <sup>+</sup> → CH <sub>3</sub> <sup>+</sup> + CH <sub>3</sub> CO	3.31	6.06	4.56	2.75	1.25	2.0 × 10 <sup>9</sup>	9.0 × 10 <sup>7</sup>	>10 <sup>-10</sup>

reaction	$\epsilon_0$	$E$		$E - \epsilon_0$		$k(E)$		$\approx \tau_k$
		CO <sub>2</sub> <sup>+</sup> c	(CO <sub>2</sub> ) <sub>4</sub> <sup>+</sup> c	CO <sub>2</sub> <sup>+</sup>	(CO <sub>2</sub> ) <sub>4</sub> <sup>+</sup>	CO <sub>2</sub> <sup>+</sup>	(CO <sub>2</sub> ) <sub>4</sub> <sup>+</sup>	
(CH <sub>3</sub> ) <sub>2</sub> CO <sup>+</sup> → CH <sub>3</sub> CO <sup>+</sup> + CH <sub>3</sub>	0.61	4.10	3.49	3.49	2.88	2.5 × 10 <sup>13</sup>	1.8 × 10 <sup>13</sup>	<10 <sup>-12</sup>
(CH <sub>3</sub> ) <sub>2</sub> CO <sup>+</sup> → CH <sub>3</sub> <sup>+</sup> + CH <sub>3</sub> CO	3.31	4.10	3.49	0.79	0.18	1.5 × 10 <sup>7</sup>	1.0 × 10 <sup>5</sup>	>10 <sup>-10</sup>

<sup>a</sup> In electron volts. <sup>b</sup> In inverse seconds, calculated from eq 3. <sup>c</sup> Species responsible for charge-transfer excitation.

Table I gives details of the range of internal energies available to a molecular ion given that it is excited by charge transfer from either an argon atom (IP = 15.79 eV) or an argon cluster (IP = 14.24 eV)<sup>24</sup>. A similar set of energy values is also given for the carbon dioxide-acetone system. Also presented in the table are the critical energies of reaction,  $\epsilon_0$ , for the two decomposition routes given above.<sup>17,18</sup> It has been assumed that isotopic substitution has a negligible effect on the ionization and appearance potentials<sup>21</sup> and that following charge transfer the inert gas atom or molecule returns to the electronic ground state. Given the narrow range of internal energies available to the molecular ion, it is possible to use the RRKM theory to place an upper and lower limit on the lifetime of the ion with respect to the two decomposition routes. These lifetimes have been calculated from the equation<sup>27</sup>

$$k(E) = \frac{\alpha \sum P(E - \epsilon_0)}{hN(E)} = \frac{1}{\tau_k} \quad (3)$$

where  $k(E)$  is the rate constant for the unimolecular decomposition of an ion with an internal energy  $E$ ,  $\sum P(E - \epsilon_0)$  is the sum of energy states in the transition state,  $N(E)$  is the density of energy states in the activated ion,  $h$  is Planck's constant,  $\alpha$  is the reaction path degeneracy, and  $\tau_k$  is the ion's lifetime. The sums and densities of energy states were calculated by using the approximation due to Whitten and Rabinovitch.<sup>28</sup> The vibrational frequencies for acetone and acetone-*d*<sub>6</sub> were selected from standard tables,<sup>29</sup> and we have made the initial assumption that the reactions proceed independent of the inert gas component. The calculated lifetimes are given in the last two columns of Table I. It can be seen from the results that for the reactions we observe the lifetimes of the ions are always <10<sup>-12</sup> s but that for reaction step 2 the calculated lifetimes are all >10<sup>-10</sup> s. If it is assumed that both of these processes are also in competition with vibrational predissociation, then it could be concluded that reaction 1 proceeds because it is faster than the latter but that vibrational predissociation is in turn faster than reaction 2. Typical predissociation lifetimes might be expected to lie in the range 10<sup>-11</sup>-10<sup>-9</sup> s.<sup>1</sup>

It was mentioned in the introduction that compared with a diatom, the increased number of vibrational degrees of freedom in a polyatomic molecule could influence the vibrational predissociation lifetime.<sup>1</sup> To test this possibility a simple model has been constructed. It is assumed that the C=O stretch of the acetone ion is the vibrational mode which is coupled most strongly to the inert gas component of the cluster and that the remainder of the molecular ion extends out from the main body. The latter part of this assumption is consistent with previous conclusions regarding the structure of these clusters, and the reason for choosing the C=O stretch will become obvious later. The limited degree of interaction between the two cluster components may prevent optimum coupling between vibrational modes from the viewpoint of an energy gap or momentum gap relationship.<sup>11-13</sup> Vibrational predissociation from the cluster is assumed to be accompanied by the propensity rule<sup>1</sup>  $\Delta\nu = -1$  ( $\omega_c(\text{C=O})$  taken as 1700 cm<sup>-1</sup>

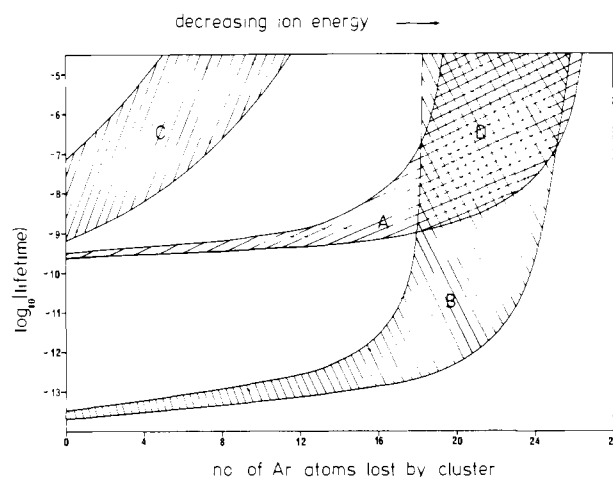


Figure 6. Variation in the lifetime of Ar<sub>n</sub>(CD<sub>3</sub>)<sub>2</sub>CO<sup>+</sup> with respect to either acetone ion decomposition or argon atom predissociation as a function of the internal energy of the ion. According to the model presented in the text, the acetone ion is assumed to lose internal energy through the evaporation of argon atoms. Region A corresponds to the predissociation lifetime, region B is the lifetime of the ion with respect to reaction 7, and region C is the lifetime of the ion with respect to reaction 8. Further details can be found in the text.

= 0.21 eV) and the departure of each inert gas atom or molecule reduces the internal energy of the ion by this amount. In this first approximation we consider predissociation to be a  $V - T$  process; it is, however, recognized that a  $V - V' + T$  process could operate on a much shorter time scale.<sup>11-13</sup> If it is further assumed that the molecular ion behaves in a statistical manner, then the probability that with an internal energy  $E$  the ion will have energy  $\omega_c$  in the appropriate degree of freedom is given by

$$P(\omega_c, E) = \frac{N_{s-1}(E - \omega_c)}{N_s(E)} \quad (4)$$

where  $s$  is the number of vibrational degrees of freedom. Obviously, predissociation will also take place if the energy in the vibrational mode is greater than  $\omega_c$ . When classical expressions for the densities of energy states<sup>27</sup> are used, it is easy to show that the probability of the C=O stretch containing an energy greater than or equal to  $\omega_c$  is given by

$$P_i(\omega_c, E) = \int_{\omega_c}^E P(\omega_c, E) dE = (1 - \omega_c/E)^{s-1} \quad (5)$$

The final expression is not unlike the RRK rate constant equation for the unimolecular decomposition of a molecule.<sup>27</sup> The predissociation lifetime for a polyatomic molecule is then taken to have the dependence

$$\frac{1}{\tau_p} = \frac{P_i(\omega_c, E)}{\tau_d} \quad (6)$$

where  $\tau_d$  is an appropriate predissociation lifetime for a diatom with an energy greater than or equal to  $\omega_c$ . For the purposes of the present calculations,  $\tau_d$  was taken as 10<sup>-10</sup> s. Figure 6 shows

(27) Forst, W. "Theory of Unimolecular Reactions"; Academic Press: New York, 1973.

(28) Whitten, G. Z.; Rabinovitch, B. S. *J. Chem. Phys.* **1963**, *38*, 2466.

(29) Benson, S. W. "Thermochemical Kinetics"; Wiley: New York, 1968.

the results from a series of calculations in which eq 3 and 6 have been used to determine the lifetime of an  $\text{Ar}_n(\text{CD}_3)_2\text{CO}^+$  cluster with respect to the reaction and predissociation channels open to it. For each predissociation event the internal energy of the molecular ion,  $E$ , has been reduced by 0.21 eV ( $\Delta\nu = -1$ ), and new decomposition rate constants and a new predissociation lifetime have been calculated. For the loss of zero argon atoms, the numbers on the graph correspond to the values given in Table I. The area on the graph labeled B corresponds to the lifetime of the ion with respect to the decomposition route



The area marked A is the vibrational predissociation lifetime, and area C is the ion's lifetime with respect to the decomposition route



Each of the calculated lifetimes is contained within a band because the initial internal energy of the ion,  $E$ , could vary according to the nature of the species responsible for charge transfer, i.e.,  $\text{Ar}^+$  or  $\text{Ar}_6^+$ . The value of  $n$  is not specified, but obviously if extensive vibrational predissociation is to occur, then it must be assumed to be quite large.

Although these calculations can only be considered as approximate, they do show a number of interesting features; firstly, it would appear that ion decomposition via reaction 7 can remain very competitive even after the loss of a substantial number of argon atoms. This point was not fully appreciated in our analysis of the argon-dimethyl ether results.<sup>16</sup> We assumed then<sup>16</sup> that once predissociation had started, the resultant energy loss would be sufficient to suppress unimolecular decomposition. Secondly, with  $\tau_d = 10^{-10}$  s, the vibrational predissociation lifetime is always less than the ion's lifetime with respect to reaction 8. However, we could reduce  $\tau_d$  by several orders of magnitude, and  $\tau_p$  would still be longer than the unimolecular lifetime for reaction 7. Finally, the region we have labeled D could be of particular interest because there decomposition and predissociation are in competition.<sup>8</sup> The normal mass spectra from our apparatus only provide ion intensities, and they do not give any direct information on the time scales of the various events taking place within the ion source. However, if an ion has a lifetime (either reactive or predissociative) within the range  $10^{-6}$ – $10^{-5}$  s, there is a high probability that it will decompose in the field-free region of the mass spectrometer and produce what is known as a metastable peak.<sup>30</sup> It can be seen from Figure 6 that both predissociation and reaction 7 could compete to produce a metastable peak; experimental confirmation of such behavior would not only make an invaluable contribution to our understanding of the predissociation mechanism, but it would also reduce the uncertainty limits on our assignment of  $\tau_d$ .<sup>31</sup> Unfortunately, the ion unimolecular reactions which normally produce the most intense metastable peaks are rearrangement processes,<sup>30</sup> and these appear to be suppressed once a molecular ion becomes associated with an inert gas cluster.<sup>14–16,22</sup> Figure 7 shows the corresponding reaction–predissociation lifetime plot for  $\text{CO}_2$  clusters. As a direct result of its lower internal energy, an acetone ion on a  $\text{CO}_2$  cluster does not have to lose as many inert gas molecules as its argon counterpart before unimolecular decomposition ceases to be competitive. This may be one reason why the relative product intensities for  $\text{CO}_2$  are lower than those for argon. Another reason could be that the vibrational modes of the  $\text{CO}_2$  molecules participate in a fast  $V - V' + T$  predissociation mechanism, which could deplete the internal energy of the acetone ions more rapidly than the  $V - T$  mechanism considered above.

From the results given in Figures 3 and 4, it can be seen that there are pronounced variations in the relative intensities of the product ions as a function of argon cluster size. In particular, the product ion intensity is high for  $\text{Ar}_{11}$  and low for  $\text{Ar}_{16}$ . Conformation of this behavior can be found in Figure 2 which

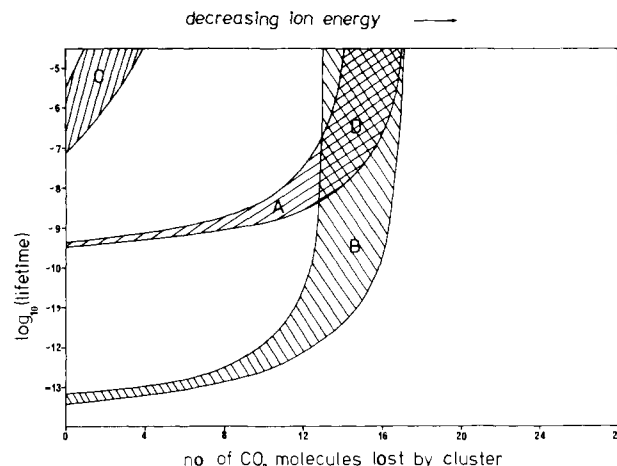


Figure 7. Same as for Figure 6 but for  $(\text{CO}_2)_n(\text{CH}_3)_2\text{CO}^+$ .

also suggests that  $\text{Ar}_{17}\text{CD}_3\text{CO}^+$  may be another high intensity combination. Similar variations were observed for the argon-dimethyl ether<sup>16</sup> system, but in that case the high intensity combinations were  $\text{Ar}_{12}\text{CHO}^+$  and  $\text{Ar}_{18}\text{CHO}^+$  and the low intensity product was  $\text{Ar}_{17}\text{CHO}^+$ . From a consideration of the dimethyl ether results and some preliminary observations on argon-diethyl ether,<sup>14</sup> it was suggested<sup>16</sup> that the high intensity product ions resulted from the ether's oxygen atom combining with the  $\text{Ar}_{12}$  and  $\text{Ar}_{18}$  clusters to give "magic" number 13 and 19 atom icosahedral configurations.<sup>32,33</sup> The remaining hydrocarbon part of the ion was then assumed to protrude out from the main body of the cluster. The available chemical evidence also supported this conclusion.<sup>14,16</sup> A similar conclusion could also be drawn from the present results if it is assumed that the  $\text{C}=\text{O}$  group of either  $\text{CD}_3\text{CO}^+$  or  $\text{CH}_3\text{CO}^+$  becomes an active constituent of the cluster's structure. The relatively high product ion intensities of  $\text{Ar}_{11}\text{CD}_3\text{CO}^+$  and  $\text{Ar}_{11}\text{CH}_3\text{CO}^+$  could then be attributed to the formation of magic number 13 atom combinations. As yet we have no satisfactory explanation for the low relative intensities of  $\text{Ar}_{16}\text{CD}_3\text{CO}^+$  and  $\text{Ar}_{16}\text{CH}_3\text{CO}^+$ . The absence of any pronounced intensity fluctuations in the  $(\text{CO}_2)_n(\text{CH}_3)_2\text{CO}^+$  system provides indirect support for the above picture, in that  $\text{CO}_2$  clusters themselves show no evidence of having any magic number configurations.<sup>34,35</sup> Finally, the proposal that the  $\text{C}=\text{O}$  group forms an active part of a cluster's structure is also supported by the chemistry of the argon-acetone system. In the mass spectrum of isolated acetone  $\text{CH}_3^+$  is quite abundant, but  $\text{Ar}_n\text{CH}_3^+$  is not observed as a product from ion cluster fragmentation. If our assumption regarding the structure of the clusters is correct, then the formation of  $\text{Ar}_n\text{CH}_3^+$  would involve displacement of the  $\text{C}=\text{O}$  group from its favored position. However, given the results in Figure 6, we would like to suggest that the appearance of a product ion is determined by kinetic rather than structural considerations and that the magic number configuration arises from vibrational predissociation and atom rearrangement after the parent ion has undergone unimolecular decomposition.

## Conclusion

In this paper we have presented the results of a detailed study of the unimolecular decomposition of the acetone and acetone- $d_6$  ions in association with argon and carbon dioxide clusters. Much of the interpretation of our results has relied on the proposal that the molecular ions are excited by a charge-transfer mechanism. Unfortunately experimental difficulties have ruled out some of the earlier evidence presented to support this suggestion.<sup>16</sup> However, the upper limits placed on the unimolecular rate constants as the result of charge transfer appear to be in accordance

(32) Hoare, M. *Adv. Chem. Phys.* **1979**, *40*, 49.

(33) Echt, O.; Sattler, K.; Recknagel, E. *Phys. Rev. Lett.* **1981**, *47*, 1121.

(34) Stace, A. J.; Moore, C. *Chem. Phys. Lett.* **1983**, *96*, 80.

(35) Eiters, R. D.; Flurchick, K.; Pan, R. P.; Chandrasekharan, V. *J. Chem. Phys.* **1981**, *75*, 929.

(30) Cooks, R. G.; Beynon, J. H.; Caprioli, R. M.; Lester, G. R. "Metastable Ions"; Elsevier: Amsterdam, 1973.

(31) Stace, A. J., work in progress.

with our experimental observations. As to whether charge transfer also places a lower limit on the rate constants remains uncertain. Given that each molecular ion receives an internal energy lying somewhere between the values specified in Table I, then they would all be expected to decompose on a time scale of between  $10^{-13}$  and  $10^{-12}$  s, and no parent ions should be present. The fact that parent ions are observed means one of two things; either they are stabilized by extensive inert gas evaporation or there is an alternative mechanism, such as direct electron impact, responsible for their formation. If direct electron impact is creating low-energy ions, i.e.,  $E < \epsilon_0$ , then it could equally well produce high-energy ions, some of which might be expected to decompose to  $\text{Ar}_n\text{CD}_3^+$  or  $\text{Ar}_n\text{CH}_3^+$ . However, ions such as these are not observed. Also, because of the increased probability of hitting the argon component, direct ionization should lead to a gradual decline in the intensity of parent ions as the cluster size increases. Figures 3-5 show no evidence of such behavior. Further kinetic evidence in support of the charge-transfer mechanism will be presented in a subsequent publication.<sup>36</sup>

By considering each unimolecular decomposition as a clock, we have been able to obtain a certain degree of time resolution against which we have measured the rate of vibrational relaxation

(36) Stace, A. J., unpublished results.

from the molecular ion to the inert gas cluster. Assuming that energy relaxation is accompanied by argon atom loss from the cluster, we can equate the relaxation times with the time scale for vibration predissociation. The results from our simple model would suggest that the time scale for vibrational predissociation in argon lies in the range  $10^{-12}$ - $10^{-10}$  s. Although this time range compares favorably with the 1-20-ps range for the vibrational relaxation of guest molecules in inert gas solids and liquids,<sup>37-39</sup> it is shorter than the  $10^{-8}$ - $10^{-9}$  s suggested by Jortner et al. from a study of the vibrational relaxation of aromatic molecules in large argon clusters.<sup>40</sup> By studying a number of the cluster reactions, we hope to be able to reduce the uncertainty on the vibrational predissociation time range presented above.

**Acknowledgment.** I thank the SERC for financial support.

**Registry No.** Ar, 7440-37-1;  $\text{CO}_2$ , 124-38-9;  $(\text{CD}_3)_2\text{CO}^+$ , 666-52-4;  $(\text{CH}_3)_2\text{CO}^+$ , 34484-11-2;  $\text{CD}_3^+$ , 17030-72-7;  $\text{CH}_3^+$ , 14531-53-4;  $\text{CD}_3\text{CO}^+$ , 20063-14-3;  $\text{CH}_3\text{CO}^+$ , 15762-07-9;  $(\text{CH}_3)_2\text{CO}$ , 67-64-1;  $(\text{C-D}_3)_2\text{CO}$ , 666-52-4.

(37) Laubereau, A.; Kaiser, W. *Annu. Rev. Phys. Chem.* **1975**, *26*, 83.

(38) Hochstrasser, R. M.; Weisman, R. B. In "Radiationless Transitions"; Lin, S. H., Ed.; Academic Press: New York, 1980; p 317.

(39) Lin, S. H. *Annu. Rev. Phys. Chem.* **1975**, *26*, p 363.

(40) Amirav, A.; Even, U.; Jortner, J. *J. Phys. Chem.* **1982**, *86*, 3345.

## Mechanistic Information from Infrared Multiple Photon Decomposition. The Ethylisopropylamine Proton-Transfer System

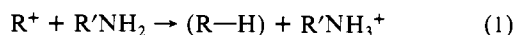
Christopher R. Moylan and John I. Brauman\*

*Contribution from the Department of Chemistry, Stanford University, Stanford, California 94305. Received July 11, 1984*

**Abstract:** Infrared multiple photon decomposition of ethylisopropylammonium ion, the putative intermediate of two different gas-phase proton-transfer reactions, has been carried out. The product distributions for both proton-transfer reactions have been determined. These have been compared with the photochemical results as well as with the high-pressure product distribution for the reaction of isopropyl cation with ethylamine. We conclude that proton transfers from carbonium ions to amines do not follow addition-elimination mechanisms even if such pathways are available. The role of the addition product in the reaction dynamics is clarified.

Determining which of several available pathways a chemical reaction follows is an inherently interesting problem in chemistry. This is just as true for gas-phase reactions as it is for solution-phase ones, although the number of different possible mechanisms for ionic reactions in the gas phase is smaller because of the absence of solvent participation. In some cases, competition can arise between multiple unimolecular reactions of a single intermediate; the outcomes of such competitions determine reaction mechanisms. Photochemical activation of putative intermediates yields product distributions that can provide information sufficient to rule out certain possible mechanisms.

There has been continuing interest in the mechanism of proton transfers from alkyl carbonium ions to alkyl amines (eq 1). This



interest stems from the interesting proposal by Bowers and co-workers that these reactions may occur via addition-elimination mechanisms rather than direct mechanisms featuring hydrogen-bound complexes, which are normally the only pathways available.

Su and Bowers<sup>1</sup> measured the rates of reaction 1 for several alkyl groups R. They found that the reactions were unit efficient for  $\text{C}_1$ - $\text{C}_3$  cations, but were as low as 60% efficient with the *tert*-butyl cation as the reactant. A subsequent study<sup>2</sup> using several different neutral species as  $\text{C}_4\text{H}_9^+$  sources produced efficiencies for proton transfer to ammonia ranging from 50 to 80%. The lower limit of this range agreed with an earlier measurement of the *tert*-butyl cation/ammonia reaction rate.<sup>3</sup> The authors proposed that tertiary carbonium ions follow a mechanism different from that of the other cations, namely, addition to form a complex  $\text{RR}'\text{NH}_2^+$  and subsequent four-center elimination to yield products. Slow proton transfers from  $\text{C}_5\text{H}_{11}^+$  formed from *n*-pentyl chloride were attributed to isomerization of the carbonium ion before reaction, yielding the tertiary species. Modeling studies

(1) Su, T.; Bowers, M. T. *Int. J. Mass Spectrom. Ion Phys.* **1973**, *12*, 347-356.

(2) Su, T.; Bowers, M. T. *J. Am. Chem. Soc.* **1973**, *95*, 7611-7613.

(3) Hellner, L.; Sieck, L. W. *J. Res. Natl. Bur. Stand., Sect. A* **1971**, *75*, 487-492.